

# Toward Constraintless Time-Correlated Single-Photon Counting Measurements: A New Method to Remove Pile-Up Distortion

Ivan Rech , Senior Member, IEEE, Angela Bovolenta , Graduate Student Member, IEEE, Alessandro Cominelli , and Giulia Acconcia , Member, IEEE

**Abstract**—Time-Correlated Single-Photon Counting (TCSPC) is a well-renowned technique allowing to reconstruct light signals with high sensitivity and resolution. Nevertheless, to this day, its use in applications requiring a fast analysis of the sample is limited due to its long acquisition time. The reason is twofold: on one hand, it is based on a statistical method thus requiring the collection of a large number of events to properly reconstruct the signal waveform; on the other hand, the average number of photons impinging on the sensor has to be kept particularly low to avoid artifacts. Indeed, the existence of dead time of both single-photon detectors and electronics can lead to distortion in the reconstructed waveform, which can be mitigated only if the count rate is kept below few percent of the excitation frequency. Recently, it has been demonstrated that an appropriate tuning of detector dead time allows to remove such power restriction, but, unfortunately, this constraint also sets a limit to the maximum count rate of the detector. In this paper, we present a novel method for TCSPC measurements, which ensures negligible distortion at unprecedented rates without requiring any constraint on either illumination power or detector dead time. We will show that this is possible thanks to the acquisition of additional information on the status of TCSPC system. The theoretical analysis reported in this paper is supported by analytical computation and numerical simulation, taking into account also potential non idealities of a real implementation.

**Index Terms**—Time-correlated single-photoncounting (TCSPC), pile-up, speed enhancement, correction algorithm.

## I. INTRODUCTION

WHEN faint and fast signals have to be measured with picosecond resolution, time-correlated single-photon counting (TCSPC) is one of the techniques of election. Thanks to its non-invasive nature, it has gained importance in life sciences, where the analysis of fluorescence phenomena can give specific and functional information about the sample. For instance, biochemical parameters of the micro-environment such as pH,

Manuscript received 28 April 2023; revised 7 August 2023; accepted 25 September 2023. Date of publication 2 October 2023; date of current version 15 December 2023. (Corresponding author: Angela Bovolenta.)

Ivan Rech, Angela Bovolenta, and Giulia Acconcia are with the Department of Electronics, Information and Bioengineering of the Politecnico di Milano, 20133 Milan, Italy (e-mail: ivan.rech@polimi.it; angela.bovolenta@polimi.it; giulia.acconcia@polimi.it).

Alessandro Cominelli is with the Tecnosens S.P.A., 25125 Brescia, Italy (e-mail: alessandro.cominelli@polimi.it).

Color versions of one or more figures in this article are available at <https://doi.org/10.1109/JSTQE.2023.3321293>.

Digital Object Identifier 10.1109/JSTQE.2023.3321293

oxygen content, viscosity, ions concentration and many other can be measured quantitatively [1] by means of fluorescence lifetime imaging microscopy (FLIM), which is based on TCSPC. In this case, a laser beam periodically excites the sample under test and the re-emitted photons are detected through a single photon detector. Historically, photo multiplier tubes (PMT) were used, but thanks to advances in single photon avalanche diode (SPAD) technology, they have been gradually replaced by the latter [2]. Every time a photon is detected, a dedicated timing circuit (such as a Time-to-Amplitude or a Time-to-Digital Converter) measures its time of arrival with respect to the laser pulse. This information is saved by the elaboration unit (usually a field programmable gate array, FPGA) and it is used to build a photon arrival time histogram, which, at the end of the experiment, will have the same shape of the fluorescence signal produced by the sample [3]. The waveform of interest is thus reconstructed in a statistical way, meaning that a large number of samples has to be collected in order to limit the committed error. The repetitive nature of TCSPC can easily lead to a long acquisition time. To surpass this limitation, in principle the intensity of illumination could be raised to obtain a high number of events in a short time interval. Unfortunately, this is not a viable solution. Indeed, the presence of a finite dead time of both detector and conversion electronics prevents the recording of all events in a real system, easily leading to distortion on the reconstructed waveform. More precisely, there are three sources of distortion [3], [4]: classic pile-up, conversion dead time pile-up, and detector dead time pile-up. Classic pile-up derives from the impossibility for the system to acquire more than one event in each excitation period, meaning that only the first detected photon is processed, while the following ones are systematically discarded. On the other hand, conversion and detector dead time pile-up originate from the fact that both single-photon detectors and conversion electronics typically require some time to process one event and during this time interval (so-called dead time) they are insensitive to any other stimulus. While classic pile-up and conversion dead time pile-up could be significantly mitigated by recently-developed multi-hit [5] and high-speed converters [6], the main limitation is currently due to the finite dead time of the detector. Considering the exploitation of a SPAD, for example, its dead time is controlled by means of a specific circuit, known as active quenching circuit (AQC). In the last few years, AQC architectures have been proposed

to minimize the dead time, exploiting both high-performance custom detectors [7] or integrated CMOS SPADs [8], [9], [10], achieving in this field a dead time of few nanoseconds [11] or even below 1 ns [10]. In addition, new hybrid photodetectors have been presented as an alternative to SPADs, offering a pulse duration of few nanoseconds and thus enabling high count rates [12]. Unfortunately, even a short dead time can easily lead to distortion in TCSPC if the illumination power is too high. For this reason, a classic solution to avoid pile-up distortion consists in limiting the average number of photons per period to be far less than one, resulting in a maximum count rate of the single acquisition channel equal to only a few percentage of the excitation rate (typically 1% to 5%). For example, with a typical excitation rate of 80 Mcps, the speed of the single TCSPC acquisition channel is limited to a few Mcps. The main workaround to this limitation has relied on the development of multichannel systems. Assuming to have  $N$  channels, the overall system counting capability is expected to increase by the same factor. To this attempt, many multichannel systems based on SPAD arrays have been presented in literature [13], [14], [15]. However, despite their high potential, the large amount of data potentially generated by dense SPAD arrays cannot be fully extracted because of the limited bandwidth towards the external elaboration unit, thus the real speed increment is lower than a factor  $N$  [4]. Unfortunately, the development of efficient read-out architectures able to fulfil the requirements of variegated TCSPC measurement scenarios is still an open challenge mainly due to implementation complexity [16]. A real turning point was made in 2017, with the introduction of a new solution [17], which aims at removing pile-up distortion and the power constraint deriving from it. In particular, it was demonstrated that matching the detector dead time with an integer multiple of the laser period leads to have a distortion lower than 1%, whatever the illumination power is. In this way, the operating speed of a single acquisition channel can be increased. In [18] a speed increment by a factor 8 with respect to classic TCSPC systems has been experimentally demonstrated with a single-channel SPAD-based system, a solution that can be extended to a multichannel system to further increase the system speed. Nevertheless, the necessity to fix a dead time value to prevent distortion intrinsically forces a limit to maximum speed, since dead time cannot be further reduced. The problem of distortion can be managed differently: it can be corrected at the end of the experiment, leveraging some fitting algorithms, such as least square method (LSM) or maximum likelihood (ML). An interesting example is presented in [19]. The correction method adopted not only uses LSM or ML, but it also incorporates losses of events due to pile-up, removing deterministic errors otherwise present. Unfortunately, to be fully effective it needs to know in advance the shape of the signal, which is not the case in most of real cases.

In this article, we present a novel approach to carry out distortionless TCSPC measurement without any constraint. We will show that combining information about the status of the system with the classic TCSPC histogram, the reconstructed fluorescence signal features near-zero distortion, even though there are no restrictions on illumination power and detector dead time. The method does not require any a priori knowledge of the

signal shape and the acquisition speed of the single channel can experience a significant increase. All existing limitations are removed, opening the way to the development of constraint-less TCSPC single and multi-channel systems.

The article is organized as follows: starting from the theory behind the reconstruction of the signal in a TCSPC experiment, a brief explanation of pile-up and counting-loss will be done in Section II. Knowing that the former is the real problem, in Section III a recently proposed solution to completely avoid it will be revised. After discussing the limits of that solution, in Section IV a novel approach will be presented, by means of mathematical computations and numerical simulations. To make the analysis exhaustive, the effect of non idealities of a real implementation will be presented as well. Finally, conclusions will be drawn in Section VI.

## II. SIGNAL RECONSTRUCTION

The idea behind TCSPC is to reconstruct a signal starting from the function which describes in time the rate of impinging photons. In general, the rate function  $r(t)$  can be defined as follows:

$$r(t) = N \cdot p(t) \quad (1)$$

where  $N$  is the mean number of events in the time interval of interest and  $p(t)$  is the probability density function (pdf) of the event. In a TCSPC experiment, (1) becomes:

$$r_{imp}(t) = \mathcal{P} \cdot p_{imp}(t) \quad (2)$$

where  $r_{imp}(t)$  is rate of impinging photons,  $\mathcal{P}$  is their mean number in a time interval equal to the laser period  $T_{laser}$ , and  $p_{imp}(t)$  is the probability density function. The pdf can have whatever shape but, for sake of simplicity, in this article the case of a single exponential decay function will be considered; the obtained results do not depend on this choice and they can be extended to a general case. In this scenario,  $r_{imp}$  can be described with the formula below:

$$r_{imp}(t) = R_0 \cdot e^{-\frac{t}{\tau}} \cdot u(t) \quad (3)$$

where  $R_0$  is a constant proportional to the power of the incident signal,  $\tau$  is the decay time constant, and  $u(t)$  is the Heaviside function, also called *step* function. It is worth underlining that the product  $r_{imp}(t) \cdot dt$  is the mean number of photons that impinge on the detector in an infinitesimally-sized interval  $dt$  centered around  $t$ . Ideally, all the photons impinging on the detector are registered in a histogram, which at the end has the same shape of  $r_{imp}(t)$ . Unfortunately, in a real system detector and conversion electronics can be both characterised by a finite dead time, i.e. a period of time during which they are not available (Fig. 1). As a consequence, photons arriving during this interval are lost and the histogram does not precisely reconstruct  $r_{imp}(t)$ . In particular, it will be proportional to the function which describes the rate of recorded photons in a laser period,  $r_{rec}(t)$ . Nevertheless,  $r_{imp}(t)$  and  $r_{rec}(t)$  are somehow linked and the rate of impinging photons can be obtained starting from the latter. Considering to be limited only by detector dead time (see Section I), the recording rate can be written as the

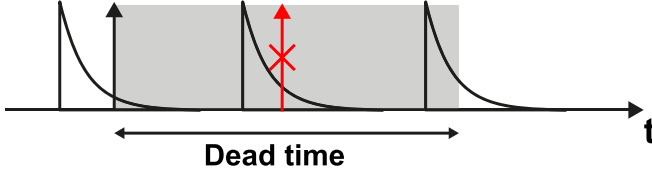


Fig. 1. Graphical representation of system dead time.

product between the impinging rate  $r_{imp}(t)$  and the probability that the system is active, namely it is able to detect photons at the time instant  $t$  of interest. Referring to [17],  $r_{rec}(t)$  can be computed as:

$$r_{rec}(t) = r_{imp}(t) \cdot \left[ 1 - \int_{t-T_{dead}}^t \sum_{i=-\infty}^{\infty} r_{rec}(t' + i \cdot T_{laser}) dt' \right] \quad (4)$$

where the summation takes into account the periodic behaviour of  $r_{rec}(t)$  and  $T_{dead}$  is the detector dead time.

The quantity between brackets can be summarized in the parameter  $\alpha$ . Thus (4) becomes:

$$r_{rec}(t) = r_{imp}(t) \cdot \alpha \quad (5)$$

Depending on whether  $\alpha$  is a constant or a function of time, two cases can be distinguished that will be discussed in the following.

#### A. Counting-Loss

Due to the presence of a finite dead time of the detector some photons are lost. As a consequence, the total number of recorded events is lower than in the ideal case, thus the counting efficiency of the system is reduced. The latter is defined as:

$$\eta = \frac{\mathcal{P}_{rec}}{\mathcal{P}} \quad (6)$$

where  $\mathcal{P}_{rec}$  and  $\mathcal{P}$  are the average number of recorded and impinging photons in a period, respectively.

Since  $\mathcal{P}_{rec}$  is always lower than  $\mathcal{P}$ ,  $\eta$  cannot be greater than one. When the probability to lose a photon is uniformly distributed within the excitation period, the shape of the reconstructed fluorescence signal is not changed and we are in presence of only *counting-loss*. In this condition, there is no loss of useful information, consequently no distortion. Referring to (4), it corresponds to considering  $\alpha$  as a constant:

$$r_{rec}(t) = r_{imp}(t) \cdot \alpha = r_{imp}(t) \cdot \eta \quad (7)$$

Clearly,  $r_{rec}(t)$  has the same shape of  $r_{imp}(t)$ , but with a reduced amplitude, thus the impinging rate can be obtained simply dividing by  $\eta$  the recording rate. To maximize the efficiency and, consequently, the measurement speed, dead time must be minimized, exploiting, for example, fast Active Quenching Circuits (AQC) with SPADs [7], [8], [9].

#### B. Pile-Up Distortion

Unfortunately, a real system does not suffer only from counting-loss and the aforementioned solution is not effective to increase the acquisition speed because of distortion due to

pile-up phenomena, as discussed in the Section I. At the beginning of each excitation cycle, the first photon impinging on the detector triggers a dead time, masking subsequent events that are unavoidably lost. At high impinging rate this happens systematically, changing the shape of the reconstructed rate  $r_{rec}(t)$  and hence introducing distortion. This effect is even more serious if the rate function has an initial peak, like in the case of an exponential: combining a reduction of  $T_{dead}$  with an increase of the illumination, the loss of photons and the distortion are enhanced. In general, the situation can be mathematically described considering a variation in time in the proportionality factor between  $r_{rec}(t)$  and  $r_{imp}(t)$ . Recalling (4), it becomes:

$$r_{rec}(t) = r_{imp}(t) \cdot \alpha(t). \quad (8)$$

Given that pile-up corrupts useful information, invalidating the analysis on the sample, it has to be avoided in any way.

Historically, the problem of pile-up has been limited keeping the number of impinging photons per period well below one, typically 0.01–0.05. This approach has become the standard for TCSPC measurement and the idea behind it does not rely on removing distortion, but on keeping it under a negligible level. Considering a widely used laser frequency of 80 MHz [3] and a count rate of 4 MHz (i.e., 5% of the excitation rate), the resulting error is limited to about 1.25% [3]. This result can be explained also referring to (4). Assuming that  $r_{imp}(t)$  is quite small, even the detection rate  $r_{rec}(t)$  is low and the integral term can be removed. Thus, even though  $\alpha$  is still function of time, it can be neglected and  $r_{rec}(t)$  approaches  $r_{imp}(t)$ :

$$r_{rec}(t) \approx r_{imp}(t). \quad (9)$$

Nevertheless, imposing a limit to the maximum count rate, the overall measurement speed is impaired. Indeed, according to statistics, to make the extracted information reliable a certain number of events have to be recorded. This means that if a constraint on the acquisition rate is posed, the time needed to reach the appropriate number of samples increases.

### III. DISTORTION-LESS RECONSTRUCTION

As seen in Section I, different solutions have been proposed to increase acquisition speed, still keeping distortion under a reasonable level. Nevertheless, none of them removes the problem of pile-up. In 2017, a novel approach was presented in the literature, which demonstrates that, thanks to a fine tuning of the detector dead time, it is possible to completely avoid pile-up distortion [17]. A dedicated system has been implemented [20] and real measurements have been performed [18] proving the effectiveness of this method.

To better understand the proposed idea, it is necessary to analyse the effect of  $T_{dead}$  on distortion. To this end, a numerical simulation has been carried out, reproducing the reconstruction of a mono-exponential decay fluorescence signal exploiting TCSPC technique. Indeed, this signal shape allows to quantify in a simple way distortion. Knowing that the latter arises when the measured time constant  $\tau_{meas}$  differs from the ideal one (i.e.,  $\tau$ ), firstly it is necessary to extract the value of  $\tau_{meas}$ . This can be done applying the center of mass method on the recorded

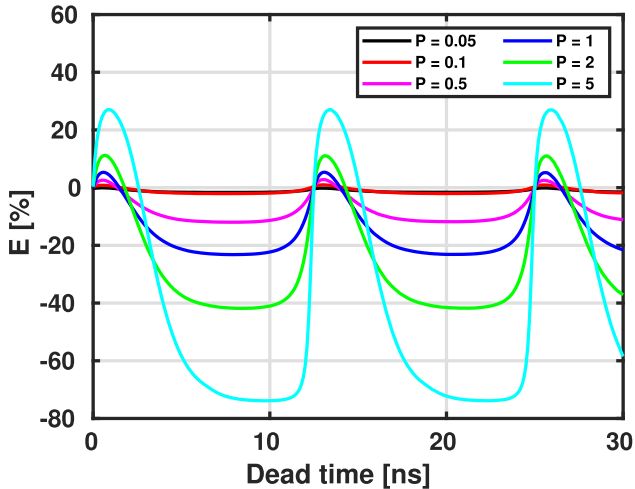


Fig. 2. Fractional estimation error  $E$  as a function of detector dead time  $T_{dead}$ , for different illumination power  $\mathcal{P}$ . Considered fluorescence time constant  $\tau = 1$  ns.

histogram:

$$\tau_{meas} = \frac{\int_0^{T_{laser}} t \cdot h(t) dt}{\int_0^{T_{laser}} h(t) dt}. \quad (10)$$

where  $h(t)$  is the recorded histogram and  $T_{laser}$  is the laser period.

Then, to quantify the degree of distortion introduced, the fractional estimation error  $E$  is computed:

$$E = \frac{\tau_{meas} - \tau}{\tau} \quad (11)$$

This process is repeated for different values of detector dead time and, at the end, the trend of  $E$  with respect to  $T_{dead}$  can be plotted. For instance, in Fig. 2 the result of a simulation is shown, for  $\tau = 1$  ns, a variable intensity of illumination  $\mathcal{P}$  and a laser period  $T_{laser}$  of 12.5 ns. As it can be observed, the error  $E$  has a periodic behaviour, with period equal to  $T_{laser}$ , and, for certain values of  $T_{dead}$ , it is zero, whatever is the intensity of illumination. In particular, this happens at integer multiples of the laser period, thus the idea is to match detector dead time with these values, in order to completely eliminate distortion [17]. For the first time, the historical limit on the rate has been removed, enabling acquisition speed to be improved overcoming the pile-up problem.

The effect just explained can be also described considering Fig. 3. When a photon impinges on the detector, it triggers a dead time equal to the laser period. At the end of this interval,  $r_{rec}(t)$  restarts from the same point it stopped in the previous period. Overall, considering the shape of  $r_{rec}(t)$ , it is like the system features no dead time and so there is no distortion.

#### A. Mathematical Demonstration

A rigorous demonstration of what has been shown graphically can be given.

In the case of a dead time equal to an integer number  $n$  of laser periods ( $T_{dead} = n \cdot T_{laser}$ ), (5) can be simplified. Indeed, the

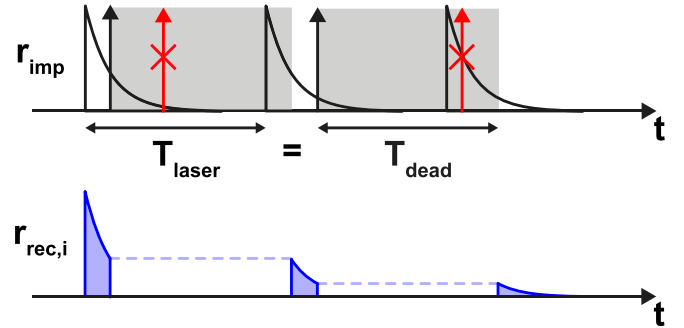


Fig. 3. Effect of a detector dead time  $T_{dead}$  equal to a laser period.  $r_{imp}$  is the impinging rate, while  $r_{rec,i}$  is the recording rate for each period. Merging all portions of  $r_{rec,i}$ , the same trend of  $r_{imp}$  is obtained.

area of the recording rate  $r_{rec}(t)$  is equal to that of the single pulse multiplied by  $n$ ; thus  $r_{rec}(t)$  becomes:

$$r_{rec}(t) = r_{imp}(t) \cdot \left[ 1 - n \cdot \int_0^{T_{laser}} r_{rec}(t') dt' \right] \quad (12)$$

The quantity between brackets is not a function of time, but it is constant. Thus, referring to (5), it is the same to consider  $\alpha$  as a constant equal to the counting efficiency  $\eta$ : the system is affected only by counting-loss. In this case  $\eta$  can be defined as follows:

$$\eta = \left[ 1 - n \cdot \int_0^{T_{laser}} r_{rec}(t') dt' \right] \quad (13)$$

This demonstrates that no distortion is affecting the measurement and the system features only counting-loss, for any illumination power.

#### B. Counting Efficiency

While the dead time matched to the laser period can avoid distortion, it still prevents the detector from registering all events, thus limiting the maximum speed of the experiment. An idea to solve the problem could be to raise the illumination power, in order to increase the overall number of photons reaching the sensor and, thus, their probability to be recorded. Unfortunately, often this is still not a viable solution because the sample could be damaged, e.g. by the so called photobleaching phenomenon [1]. In this condition, it is interesting to evaluate the mean number of recorded photons in a period as a function of the dead time  $T_{dead}$  and the power of illumination, with a particular attention to the case  $T_{dead} = n \cdot T_{laser}$ . To this aim, the integral over  $[0; T_{laser}]$  of (4) has to be computed:

$$\mathcal{P}_{rec} = \int_0^{T_{laser}} r_{imp}(t) \cdot \left[ 1 - \int_{t-T_{dead}}^t \sum_{i=-\infty}^{\infty} r_{rec}(\cdot) dt' \right] dt. \quad (14)$$

where  $\mathcal{P}_{rec}$  is  $\int_0^{T_{laser}} r_{rec}(t) dt$ .

Usually, the equation can be solved only numerically, but in case of  $T_{dead} = n \cdot T_{laser}$ , it is possible to obtain a closed form expression for  $\mathcal{P}_{rec}$ .



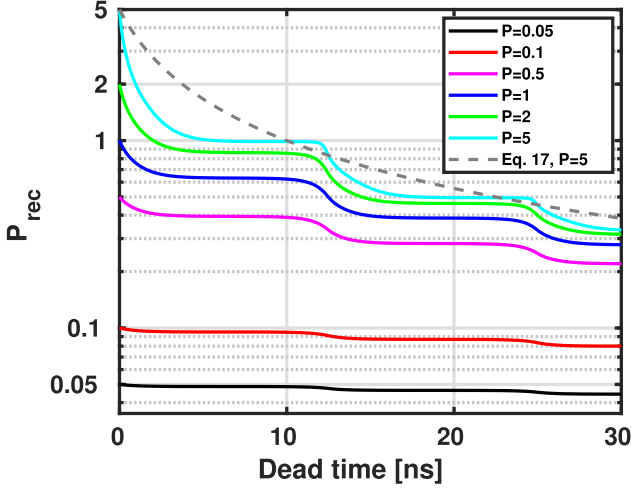


Fig. 4. Counting efficiency  $\mathcal{P}_{rec}$  as a function of detector dead time  $T_{dead}$ , for different illumination power  $\mathcal{P}$ . Considered fluorescence time constant  $\tau = 1$  ns.

Indeed, starting from (12), it results:

$$\mathcal{P}_{rec} = \mathcal{P} \cdot \left[ 1 - n \cdot \int_0^{T_{laser}} r_{rec}(t') dt' \right] = \mathcal{P} \cdot \eta \quad (15)$$

since the quantity between brackets does not depend on  $t$  and it is equal to the counting efficiency. Referring to (13), the latter can be rewritten as:

$$\eta = 1 - n \cdot \mathcal{P}_{rec}. \quad (16)$$

Substituting  $\eta$  in (15),  $\mathcal{P}_{rec}$  becomes:

$$\mathcal{P}_{rec} = \frac{\mathcal{P}}{1 + \mathcal{P} \cdot \frac{T_{dead}}{T_{laser}}}. \quad (17)$$

where  $n$  has been replaced with  $T_{dead}/T_{laser}$ .

This expression can be obtained also solving (4) for a constant illumination. Indeed, in this case, the rate functions are constant during the entire experiment and they have an area equal to  $\mathcal{P}$  or  $\mathcal{P}_{rec}$  over a laser period, allowing to solve the equation. Fig. 4 shows  $\mathcal{P}_{rec}$  as a function of the dead time, for different average number of impinging photons  $\mathcal{P}$ . Curves for pulsed illumination are plotted together with the one for constant illumination, in dashed line.

It is evident that the former decreases as a staircase. This behaviour can be explained considering the duration of  $T_{dead}$  with respect to the fluorescence signal. As long as the dead time is shorter than the signal duration,  $\mathcal{P}_{rec}$  decreases as  $T_{dead}$  increases. Conversely, if the dead time becomes longer than the signal but it does not influence the subsequent period, its increase has no effect on  $\mathcal{P}_{rec}$ , which features a plateau. When this condition does not hold anymore,  $\mathcal{P}_{rec}$  has a step down. This trend is more and more evident as the intensity of illumination is raised. Furthermore, it can be seen that for integer multiples of  $T_{dead}$  the two types of curve crosses. Nevertheless, what is really important to highlight is that  $\mathcal{P}_{rec}$  is never equal to  $\mathcal{P}$ , if a finite dead time is present. It is evident that the new approach of [17] has a limitation: in the best case, the system is forced

to wait at least for a laser period before being ready again. This means that, even though acquisition speed can be increased, the system is not exploited to its full potential.

#### IV. TOWARDS A CONSTRAINT-LESS TCSPC

A real turning point in speeding up a TCSPC measurement could be removing all existing constraints about detector dead time and intensity of illumination. However, in this way the reconstructed waveform would feature pile-up distortion and it could not be used as it is. Solutions have been proposed in literature to correct distortion using dedicated algorithms after the measurement. Unfortunately, they have some intrinsic limitations which prevent their adoption in all situations. Often, algorithms base the fitting only on the shape of the photon arrival time histogram [21], without considering additional information deriving from the system. However, this approach may be ineffective in presence of several time constants, for instance. In other cases, a model for the expected results is needed for the correction to be effective [22], limiting the field of application.

In the following a novel idea will be disclosed, in which the additional information about the status of the system enables the reconstruction of the signal, even when its shape is completely unknown.

To this end, let's come back to Section II and remember that the rate function of recorded photons  $r_{rec}(t)$  and the rate function of impinging photons  $r_{imp}(t)$  are linked through the parameter  $\alpha$ . Considering a situation in which no limitations are posed, the histogram obtained with photons arrival times is affected by pile-up distortion, thus  $\alpha$  changes with time and the relation between the two rate functions is expressed by (8). Now, if  $\alpha(t)$  is given or can be somehow reconstructed,  $r_{imp}(t)$  could be extracted simply dividing  $r_{rec}(t)$  by this function:

$$r_{imp}(t) = \frac{r_{rec}(t)}{\alpha(t)}. \quad (18)$$

At this point, a way to recover  $\alpha(t)$  is needed. The novel idea is based on the construction of another histogram representing the probability of the system to be active with a method similar to the one used in a classical TCSPC experiment, as shown in Fig. 5.

For each laser period  $T_{laser,i}$  that composes the TCSPC measurement, the status of the system is evaluated. In a general case, the system is active if detector and conversion electronics can register an impinging photon, which means that there is not an ongoing dead time, while it is blind in the other case. Every time the first condition is met, the number of counts in the corresponding  $dt$  belonging to  $T_{laser,i}$  is increased by one (the bin width  $dt$  could be in the order of tens of ps.). If the system is characterised only by detector dead time, the number of counts in the bin  $dt$  could be increased by an amount which varies between 0 and 1 with continuity. This is because, the value to be inserted corresponds to the photon detection efficiency (PDE) of the detector, which can assume a decimal value in the interval  $[0; 1]$ . Repeating this procedure at every excitation cycle, an histogram  $h_\alpha$  is created, which gives the desired probability function  $\alpha(t)$ , once it is divided by the total number of recorded

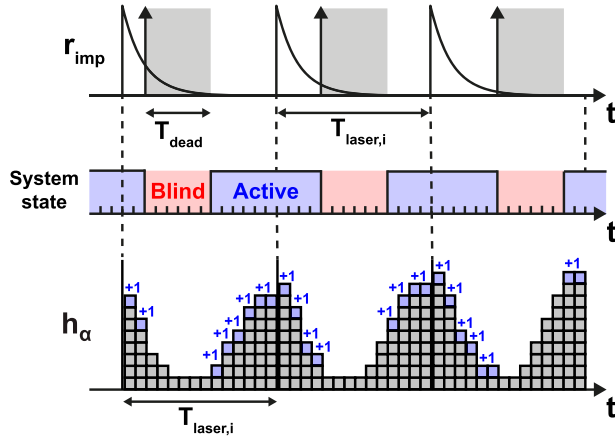


Fig. 5. Construction of the histogram representing the probability to be active  $h_\alpha$ .

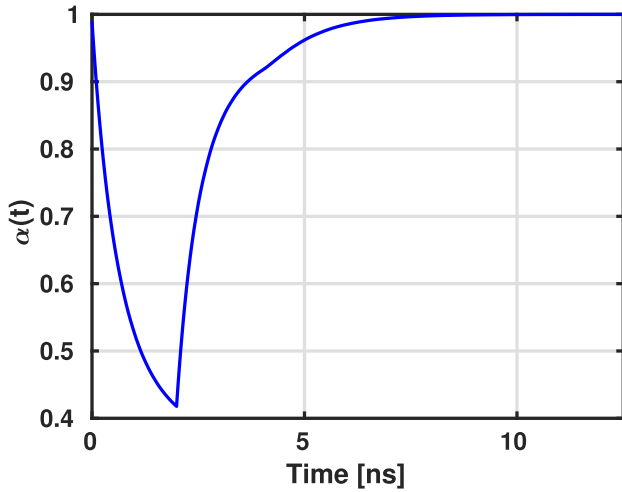


Fig. 6. Probability to be active  $\alpha(t)$  considering a time constant  $\tau = 1$  ns, a detector dead time  $T_{dead} = 2$  ns and an illumination power  $\mathcal{P} = 1$ .

counts. It is important to highlight that the method works only if it is possible to precisely measure the detector dead time, otherwise the status of the system cannot be defined correctly and the resulting histogram is not reliable. For instance, if the detector used is a SPAD, the status of the system can be recovered exploiting the AQC connected to it. Indeed, this circuit can signal the beginning and the end of the dead time, thus distinguishing between a status of activity or inactivity of the system. This information could be stored in the memory of an FPGA and it could be used to properly construct  $h_\alpha$ .

The method discussed so far has been implemented through a numerical simulation and the obtained curve of  $\alpha(t)$  is shown in Fig. 6, where a detector dead time  $T_{dead} = 2$  ns and a power of illumination  $\mathcal{P} = 1$  have been considered. In this case, bin width  $dt$  of 10 ps has been chosen. For sake of simplicity, PDE has been assumed to be either 0 or 1, excluding decimal values.

Now, combining the histogram of  $r_{rec}(t)$  and the histogram of  $\alpha(t)$ , the waveform of  $r_{imp}(t)$  is reconstructed and it features nearly zero distortion. Considering a mono-exponential decay with  $\tau = 1$  ns for the fluorescence signal, Fig. 7 shows the

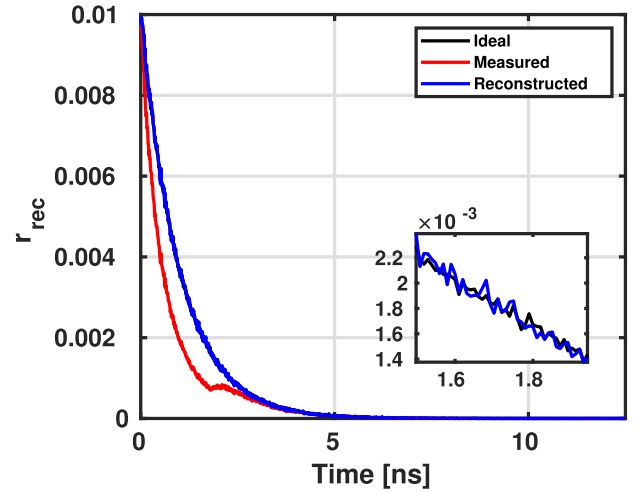


Fig. 7. Comparison between measured and reconstructed signal after the division by the function  $\alpha(t)$ , with time constant  $\tau = 1$  ns, detector dead time  $T_{dead} = 2$  ns and illumination power  $\mathcal{P} = 1$ .

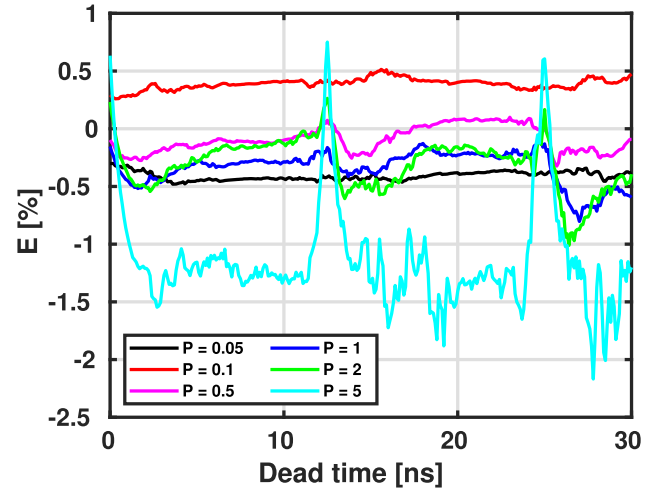


Fig. 8. Fractional estimation error  $E$  after the correction, as a function of detector dead time  $T_{dead}$ , for different illumination power  $\mathcal{P}$ .

comparison between the distorted  $r_{rec}(t)$  and the final one. It is evident that all deviations from the shape of the ideal signal are compensated and the final  $r_{rec}(t)$  perfectly follows the true signal shape, proving that the proposed method is effective. To quantify the remaining degree of distortion, the fractional estimation error  $E$  is computed for different values of detector dead time, by means of (11). As it can be seen from Fig. 8, distortion is always around that 1%, meaning that the limit of  $E = 1.25\%$ ; imposed by classic TCSCP is never overcome [3], regardless of the illumination power. Even though the dead time cannot be completely removed, the acquisition speed can be raised, because it is possible to exploit all dead time values including those in the range  $[0; T_{laser}]$ .

## V. NON IDEALITIES

The real nature of the system introduces several non idealities that can affect  $\alpha(t)$ , consequently changing the shape of the

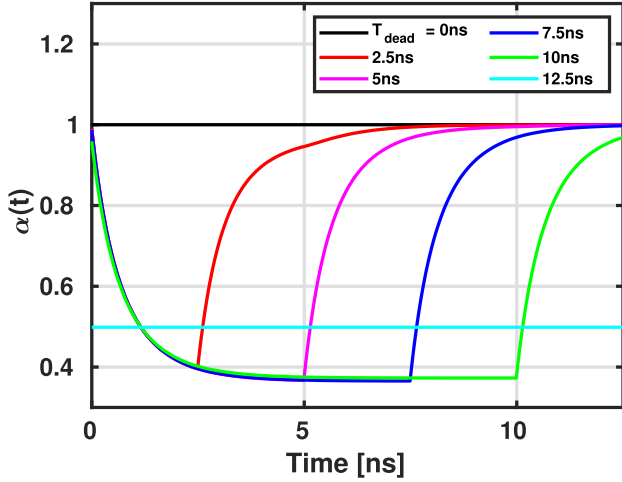


Fig. 9. Probability to be active  $\alpha(t)$  for a detector dead time  $T_{dead}$  which varies from 0 ns to 12.5 ns. Considered time constant  $\tau = 1$  ns and illumination power  $\mathcal{P} = 1$ .

reconstructed signal. Indeed, the latter is obtained from  $r_{imp}(t)$ , which is the result of the division of  $r_{rec}(t)$  by  $\alpha(t)$ . Thus, any deviation of measured  $\alpha(t)$  from its true shape can impact negatively on the impinging rate function shape.

In the following, main non idealities will be discussed, always considering a dead time belonging to  $[0; T_{laser}]$ . The obtained results are valid even for a longer  $T_{dead}$ , but we focus on the aforementioned interval because it is where this solution can be a true game changer and thus the most likely case for a future real implementation.

#### A. Minimum of $\alpha(t)$

The probability to be active  $\alpha(t)$  needs a particular attention, being the key element underlying the new proposed approach. Specifically, the dependence of its shape on detector dead time, illumination power and fluorescence time constant has to be analysed.

First, the effect of  $T_{dead}$  is considered, which is shown in Fig. 9. At the beginning, the probability to be active is high. This can be explained considering how this function is obtained: at the end of each excitation period, it is unlikely to have an impinging photon, thus the histogram is frequently updated with a new count, making the initial value quite high. Then, entering the new  $T_{laser}$ , several photons start to impinge on the photodetector, triggering a dead time and drastically reducing the probability to be active, which reaches a minimum. The longer is the dead time, the higher is the period of inactivity, which results in the creation of a plateau of  $\alpha(t)$ . Once the dead time ends, the curve comes back to the initial value. What is interesting to observe is that in all cases  $\alpha(t)$  is characterised by a minimum. This demonstrates that the system is affected by pile-up: the high photon rate in the initial part of the excitation period causes the system to be immediately blind, making secondary photons unlikely to be recorded and distorting the reconstructed signal. If  $T_{dead}$  is equal to  $T_{laser}$ , the probability to be active becomes constant again, proving that in this condition only

counting-loss arises. Referring to Fig. 9, the value of  $\alpha(t)$  reached in this condition can be computed remembering that this function becomes equal to the counting efficiency  $\eta$ . Hence, the result is:

$$\eta = \frac{1}{1 + \mathcal{P}} \quad (19)$$

where this expression is derived from (17), imposing  $T_{dead} = T_{laser}$ .

Substituting  $\mathcal{P} = 1$  in the equation,  $\eta = 0.5$  as in the plot.

It is worth mentioning that for any dead time beyond  $T_{laser}$ ,  $\alpha(t)$  shows the same trend but shifted downwards. Indeed, the system is less prone to be active, being for the majority of the time unavailable. Before going on, it is worth highlighting that  $\alpha(t)$  could be seen as an index of distortion: if its shape changes with time it means that the system is affected by pile-up and the reconstructed waveform for sure will be distorted. On the contrary, if it is constant, only counting-loss is present and distortion is null.

A similar analysis can be done by varying the illumination power and the value of the time constant  $\tau$ . Fig. 10 shows the effect of these parameters on  $\alpha(t)$ , with a fixed dead time of 2 ns. In Fig. 10(a),  $\tau = 1$  ns has been chosen. It is evident that the higher the average number of impinging photons, the lower the minimum of  $\alpha(t)$ . Indeed, increasing  $\mathcal{P}$ , the probability for the system to record an event increases in the first part of the excitation cycle, consequently reducing the probability to be active right after that. Moreover, as the photon rate rises, new minima appear, as it can be observed from the curve for  $\mathcal{P} = 5$ . On the other hand, Fig. 10(b) shows a different behaviour of the system when the time constant changes from 1 ns to 2.5 ns and  $\mathcal{P} = 1$ . As  $\tau$  increments, the minimum is shallower and larger. The phenomenon can be explained referring to Fig. 11(a). Since the area of the curves must be the same, its initial value is a function of the time constant and it is different for the two signals, specifically it is lower for the curve with  $\tau = 2.5$  ns. This means that, in the first time bins, it is more unlikely to detect a photon, resulting in an increased probability for the system to be active. Overall, it is important to highlight that the shape of  $\alpha(t)$  strongly depends on the working condition and it is not known in advance, hence it must be reconstructed during the experiment.

Another aspect that it is interesting to evaluate is the effect of  $\alpha(t)$  on the noise. Comparing the histogram of the probability to be active (Fig. 6) with the one of  $r_{rec}$  (Fig. 7), it can be clearly seen that the former is characterised by a lower noise, even difficult to observe. It means that it does not introduce any significant contribution to the overall noise during the reconstruction process (i.e., the division of  $r_{rec}(t)$  by  $\alpha(t)$ ). This is due to the large number of events collected in the histogram  $h_{\alpha(t)}$  during a TCSPC measurement, since it is updated more frequently. Nevertheless, the histogram of  $r_{rec}(t)$  is quite noisy both before and after the correction. This is due to the lower number of samples collected, which makes the noise derived from the statistics of light more relevant. Indeed, starting from  $r_{rec}(t)$ , the division is able to reconstruct the global trend of  $r_{imp}(t)$ , but it cannot compensate for the poor statistics of the recorded rate function. Moreover, there is a correlation between

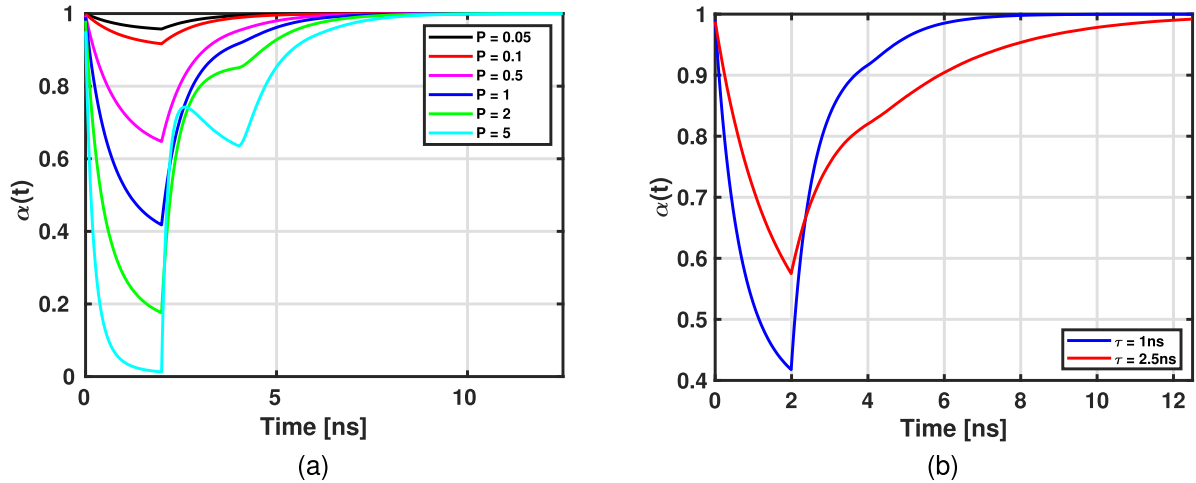


Fig. 10. Dependence of  $\alpha(t)$  with respect to the illumination power  $\mathcal{P}$  (a) and the fluorescence time constant  $\tau$  (b), for a detector dead time  $T_{dead} = 2$  ns. In (a), a time constant  $\tau = 1$  ns has been considered, while in (b) an illumination power  $\mathcal{P} = 1$  has been used.

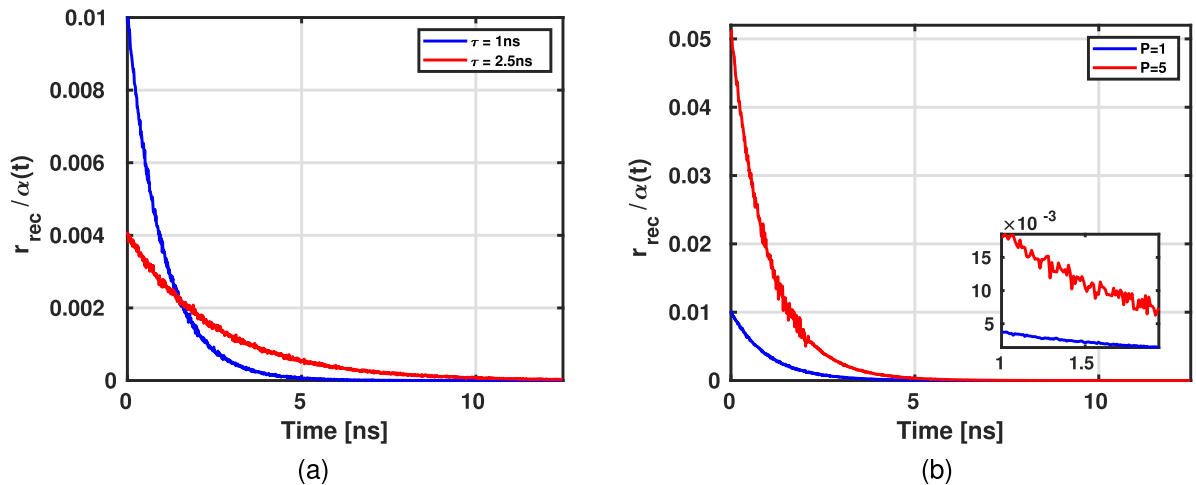


Fig. 11. In (a), the reconstructed signals for different time constant  $\tau$  and an illumination power  $\mathcal{P} = 1$ . In (b), the reconstructed signals for an illumination power of  $\mathcal{P} = 1$  and  $\mathcal{P} = 5$ . In both cases a detector dead time  $T_{dead} = 2$  ns has been considered.

the depth of the minimum in  $\alpha(t)$  and the noise of  $r_{rec}(t)$ : lower is the value reached by  $\alpha(t)$  and higher is the noise. The phenomenon can be clearly observed by increasing the power of illumination. In this condition, the system is often blind, reducing the number of photons that can be recorded, unavoidably worsening the statistics. For instance, let's compare the signals obtained after the correction for  $\mathcal{P} = 5$  and  $\mathcal{P} = 1$ , shown in Fig. 11(b). It is evident that the curve for  $\mathcal{P} = 5$  is characterised by a higher noise with respect to the curve for  $\mathcal{P} = 1$ , which is a consequence of the deeper minimum of  $\alpha(t)$ , visible from Fig. 10(a). This effect can be explained also referring to (2): a small value of  $\alpha(t)$ , corresponds to an overall amplification of  $r_{rec}(t)$ , meaning that also the superimposed noise is enhanced. A solution to the problem could be to perform gated measurements in correspondence of the minimum. Specifically, the detector could be selectively activated when it is expected to have the minimum, in order to acquire a larger number of samples in this time interval and thus reducing noise.

## B. Dead Time Errors

Dead time measurement could be affected by a deterministic error and a statistical error, i.e. the so called *jitter*. Unavoidably, the shape of  $h_\alpha$  changes and, in turn,  $r_{imp}(t)$  is modified.

This is a problem because a fundamental prerequisite for the proposed approach to be effective is the capability to precisely measure the detector dead time  $T_{dead}$ . Indeed, knowing that there is an ongoing dead time and how much it lasts, enables the update of the histogram of  $\alpha(t)$  in accordance. If this is not the case, distortion arises and the extracted information is no longer reliable. In our simulator we introduced, at first, a deterministic error of 200 ps with respect to the nominal value of  $T_{dead}$ . In Fig. 12, a nominal value of 2 ns for the dead time has been chosen, but the measured  $T_{dead}$  is 1.8 ns. In this situation, the measured  $\alpha(t)$  appears to be shifted with respect to the ideal curve. Nevertheless, focusing on the estimation error  $E$ , the use of a correction method seems to be effective since curves are still centered around 0 (except for very high illumination



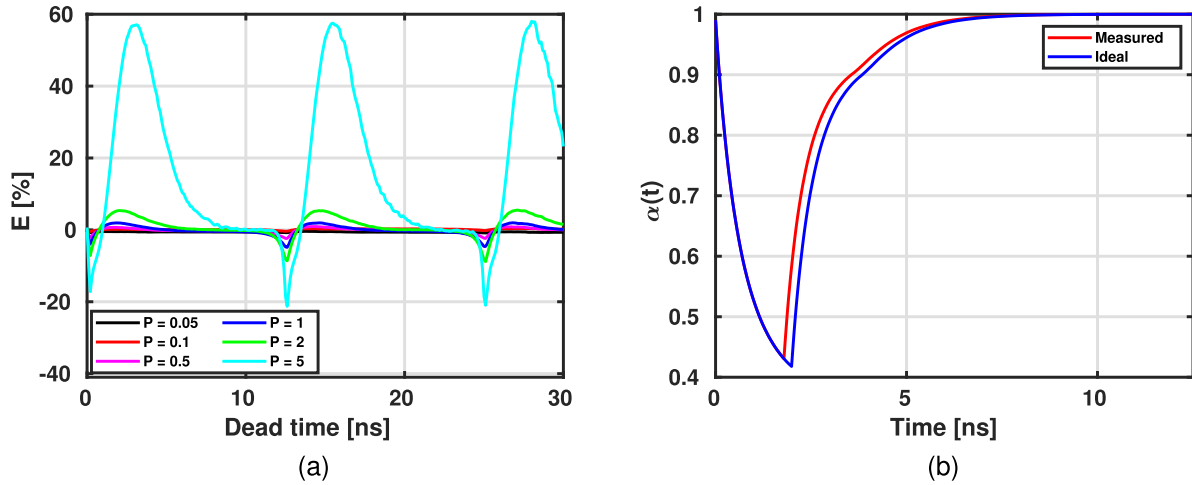


Fig. 12. Effect of a deterministic error of 200 ps in the measure of detector dead time  $T_{dead}$ . In (a), the fractional estimation error  $E$  after the correction with the estimated function  $\alpha(t)$ . In (b), the comparison between the ideal  $\alpha(t)$  and the measured function. As expected, the latter is shifted backward due to the reduced detector dead time  $T_{dead}$ . Curves are obtained for a time constant  $\tau = 1$  ns, an illumination power  $\mathcal{P} = 1$  and a dead time  $T_{dead} = 2$  ns.

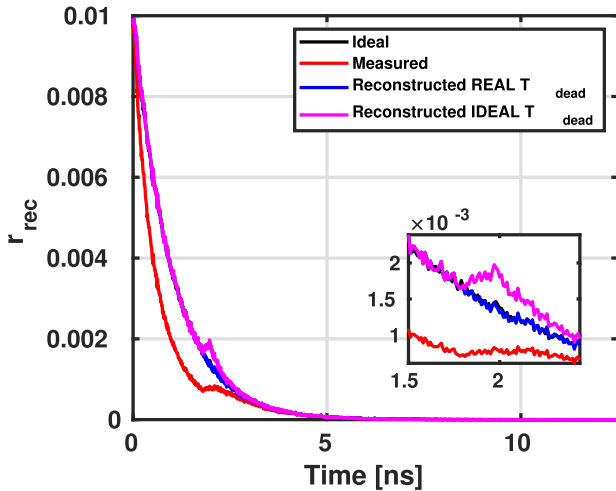


Fig. 13. Distortion in the reconstructed waveform due to the correction with the ideal curve of  $\alpha(t)$ , when there is a deterministic error of  $T_{dead}$  of 200 ps. Even though the fractional estimation error  $E$  is low, there is a visible deviation from the ideal trend. A time constant  $\tau = 1$  ns and illumination power  $\mathcal{P} = 1$  have been considered in this case.

power). Instead, analysing the shape of the reconstructed signal, sometimes it is severely distorted, even though the computed error is low. For instance, considering an illumination power  $\mathcal{P} = 1$ , the expected error is only 2%, but observing the reconstructed signal is quite distorted compared with the ideal one (Fig. 13). This depends on the method used to estimate  $\tau_{meas}$ . Indeed, exploiting a different approach with respect to the center of mass, the final error  $E$  could be higher and in accordance with the observed signal shape.

It is also worth to underline that if the system is able to measure the deviation from the nominal  $T_{dead}$ , the fluorescence waveform is not impaired. Now, let's consider a situation in which  $T_{dead}$  randomly changes from one detected photon to another. These fluctuations around the mean value can be modelled as

a statistical variable following a Gaussian distribution with a certain standard deviation  $\sigma$ . Considering an AQC operating a  $50\text{-}\mu\text{m}$  custom SPAD, the maximum measured dead time jitter is 90 ps rms [23], hence a reasonable value for this parameter to be used in simulation is 100 ps rms. Similarly to what has been observed for the deterministic error, only when intensity of illumination becomes quite high dead time jitter causes distortion to drastically increase, while in all other cases it does not have an appreciable effect (Fig. 14).

Overall, whenever the measured dead time is different from the nominal value for various reasons, but it is possible to measure its drift, the reconstruction process is not impaired.

### C. Finite Dead Time Transitions

Up to now, an ideal dead time has been considered. This means that its characteristic transitions are thought to be instantaneous, resulting in a rectangular dead time window. In a real system, these transitions are smoother and the reconstructed waveform could suffer from it. As a case study, consider a SPAD detector, which is characterised by a quench and a reset phase [24]. The latter is the most critical, because the detector becomes active again but its performance changes over time, since the bias voltage is restored gradually. Indeed, due to the reduced overvoltage across the SPAD, the ability of a photon to trigger an avalanche is reduced, resulting in a lower PDE and a delayed recording of the event [25]. Obviously, this can introduce errors in  $r_{rec}(t)$  and  $\alpha(t)$  histogram, that can cause distortion to increase.

In order to study this phenomenon a gradual change of the PDE and the timing delay has been simulated, using two types of curves with a complementary trend: as PDE increases, the delay decreases. At first, a linear variation of these quantities has been considered. Although this is an unrealistic shape, it represents a simple case to start with. It has been chosen a variation from 500 ps to 0 ps for the delay, while PDE changes from 0 to 1. The

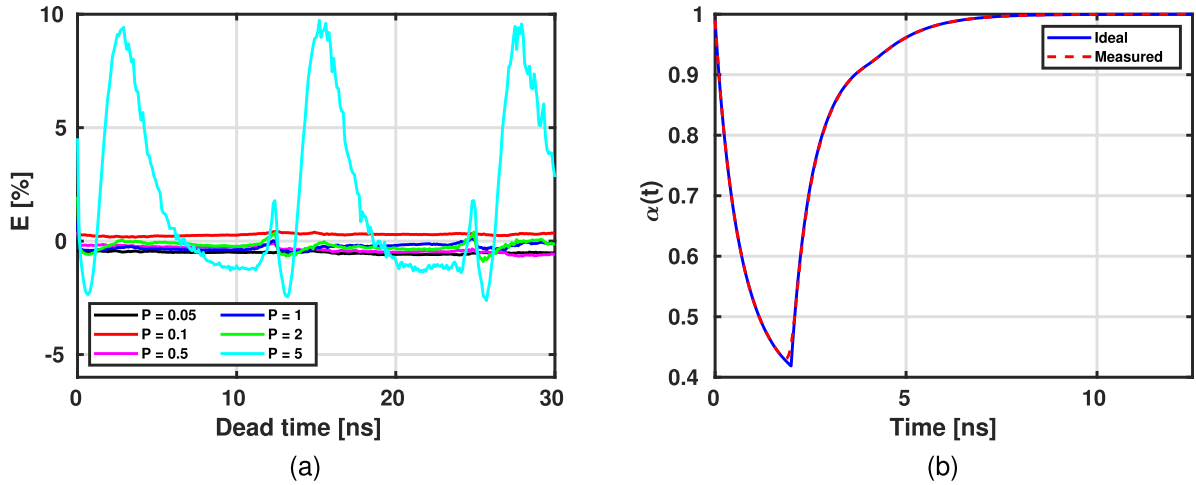


Fig. 14. Effect of a jitter of 100 ps *r.m.s.* of the value of detector dead time  $T_{dead}$ . In (a), the fractional estimation error  $E$  after the correction with the estimated function  $\alpha(t)$ . In (b), the comparison between the ideal  $\alpha(t)$  and the measured function for a time constant  $\tau = 1$  ns, an illumination power  $\mathcal{P} = 1$  and a dead time  $T_{dead}$  around 2 ns. The curves perfectly overlap, meaning that the effect of the jitter is negligible.

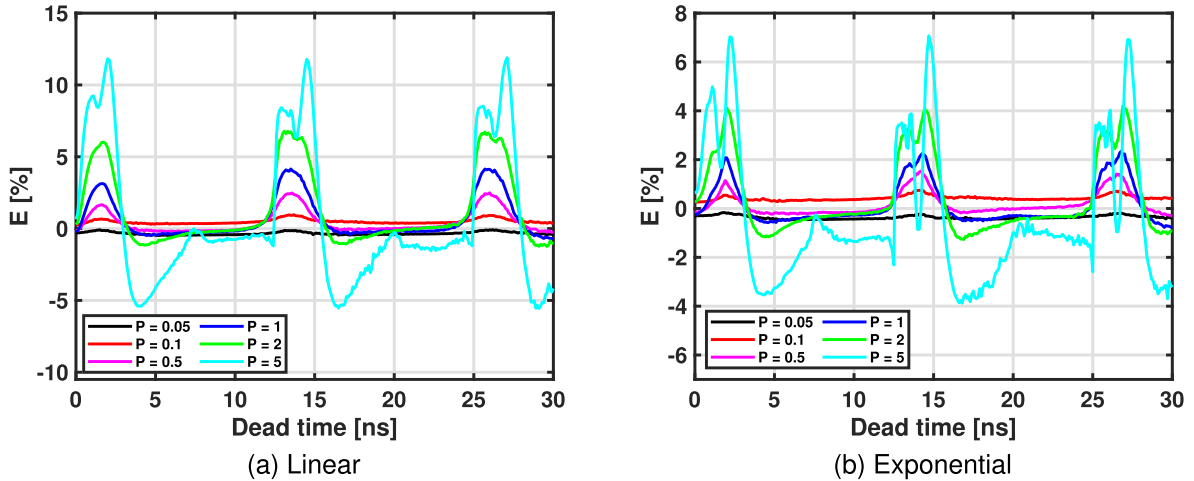


Fig. 15. Fractional estimation error  $E$  as a function of detector dead time  $T_{dead}$ , for variable illumination power  $\mathcal{P}$ , when there is a timing error in the recording of reset events. In (a),  $E$  considering a linear variation of both PDE and timing shift. In (b),  $E$  considering an exponential variation of both PDE and timing shift. In the second case,  $E$  is lower. A finite reset time of 2 ns has been considered.

resulting fractional estimation error  $E$  is shown in Fig. 15(a), together with the histogram of  $r_{rec}(t)$  and  $r_{imp}(t)$ , for a reset period lasting for 2 ns.

It is immediate to note that distortion drastically increases for low and high dead times, while for values in the middle it is not significantly influenced. The reason is that, in the latter case,  $T_{dead}$  is not long enough to cover the entire fluorescence signal, but it expires in its last part, where events are rare, thus the probability to record a photon during the reset is small and this finite transition has no effect. Then, a more realistic situation has been analysed, in which both delay and PDE have an exponential variation. As can be observed from Fig. 15(b), the only difference with respect to the previous case is the lower value reached by the error, meaning that the linear trend of both PDE and the delay leads to an overestimation of the distortion.

To make our analysis exhaustive, it must be considered also the case in which the timing information of photons in the reset phase is correctly extracted, meaning that the recording delay is zero. In this condition, if the system does not consider the presence of a finite reset time, distortion becomes quite high, even though there are no timing errors, as it is shown in Fig. 16(a). This is due to the fact that the obtained  $\alpha(t)$  substantially differs from the ideal one, thus distortion correction is not fully effective. On the contrary, if the shape of the PDE during the reset transition is known or it can be reconstructed, the histogram  $h_\alpha$  can be updated in accordance (Section IV) and distortion becomes negligible, as it can be observed from Fig. 17.

In conclusion, the effect of this non ideality could be removed provided that the duration of the reset transition is correctly measured and timing errors are corrected.

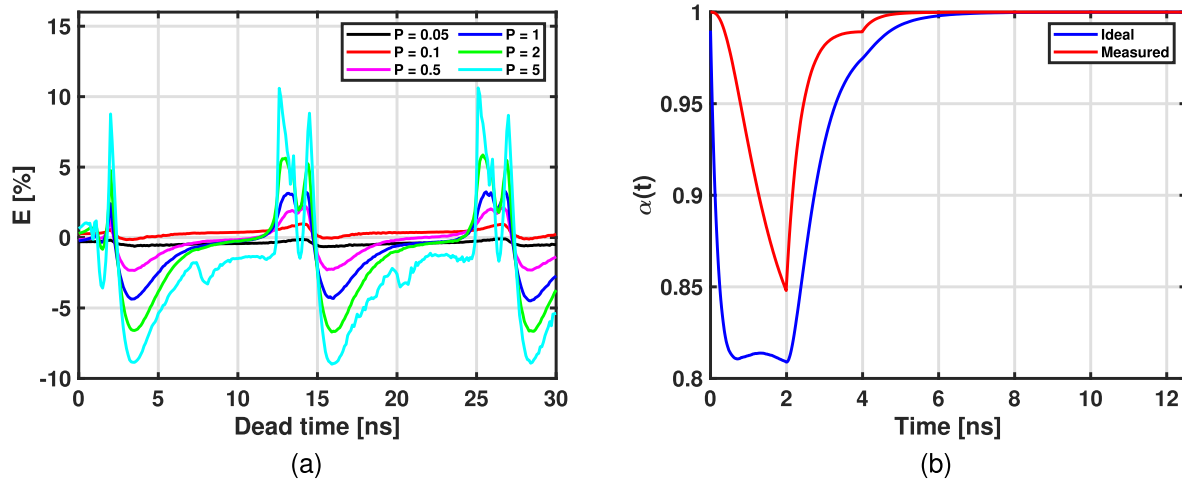


Fig. 16. Fractional estimation error  $E$  as a function of detector dead time  $T_{dead}$ , for variable illumination power  $\mathcal{P}$ , when there is not a timing error in the recording of reset events. An exponential variation for the PDE is considered. In (a), resulting  $E$  when a finite reset time is not considered during the construction of  $\alpha(t)$ . In (b), the probability to be active  $\alpha(t)$  considering or not the presence of a finite reset time.

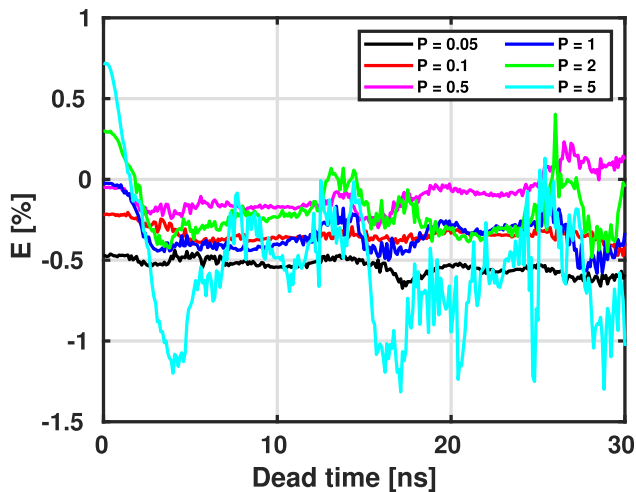


Fig. 17. Fractional estimation error  $E$  as a function of detector dead time  $T_{dead}$ , for variable illumination power  $\mathcal{P}$ , when there is not a timing error in the recording of reset events and a finite reset transition is considered in  $\alpha(t)$ .

## VI. CONCLUSION

The study of fluorescence signals in biology and medicine has become of great interest in recent years. To this aim, a technique capable of reconstructing faint signals with high resolution and sensitivity is needed; this is the case of Time Correlated Single-Photon Counting (TCSPC). Although it has several advantages with respect to analog techniques [3], it has been historically characterised by long acquisition times, preventing its use in those applications where real time analysis is requested. In addition, the necessity to avoid pile-up distortion, keeping the photon rate under a reasonable level, worsen the situation and makes it necessary to find a solution. This article, at first, reviews a solution proposed in 2017 [17]. By matching the detector dead time with an integer multiple of the laser period, pile-up distortion is completely removed for whatever photon rate, allowing to increase by almost an order of magnitude the speed of the single acquisition channel. Nevertheless, measurement velocity is still limited by a dead time equal at least to a laser period. At this point, a new groundbreaking method is presented, which guarantees near zero distortion, whatever is the photon rate

and the detector dead time. The idea is to acquire additional information on the system status and use it to correct pile-up effect in the data histogram. The new constraint-less TCSPC opens the way to unprecedented speed and performance with dedicated systems.

## ACKNOWLEDGMENT

The authors would like to thank Francesco Malanga for his precious support during the writing of this article. The system able to implement the proposed idea is an international patent pending: rif. IB2023/051995.

## REFERENCES

- [1] X. Liu et al., "Fast fluorescence lifetime imaging techniques: A review on challenge and development," *J. Innov. Opt. Health Sci.*, vol. 12, no. 5, Jul. 2019, Art. no. 1930003.
- [2] M. Ghioni, A. Gulinatti, I. Rech, F. Zappa, and S. Cova, "Progress in silicon single-photon avalanche diodes," *IEEE J. Sel. Topics Quantum Electron.*, vol. 13, no. 4, pp. 852–862, Jul./Aug. 2007.
- [3] W. Becker, *Advanced Time-Correlated Single-Photon Counting Techniques*, (Series Chemical Physics), vol. 81, A. W. C. Jr., J. Toennies, and W. Zinth, Eds. Berlin, Germany: Springer, 2005.
- [4] J. Arlt et al., "A study of pile-up in integrated time-correlated single photon counting systems," *Rev. Sci. Instrum.*, vol. 84, Oct. 2013, Art. no. 103105.
- [5] P. Peronio, G. Acconcia, I. Rech, and M. Ghioni, "Improving the counting efficiency in time-correlated single-photon counting experiments by dead-time optimization," *Rev. Sci. Instrum.*, vol. 86, Nov. 2015, Art. no. 113101.
- [6] R. Machado, J. Cabral, and F. S. Alves, "Recent developments and challenges in FPGA-based time-to-digital converters," *IEEE Trans. Instrum. Meas.*, vol. 68, no. 11, pp. 4205–4221, Nov. 2019.
- [7] F. Ceccarelli, G. Acconcia, A. Gulinatti, M. Ghioni, and I. Rech, "Fully integrated active quenching circuit driving custom-technology SPADs with 6.2-ns dead time," *IEEE Photon. Technol. Lett.*, vol. 31, no. 1, pp. 102–105, Jan. 2019.
- [8] F. Gramuglia, M.-L. Wu, C. Bruschini, M.-J. Lee, and E. Charbon, "A low-noise CMOS SPAD pixel with 12.1Ps SPTR and 3Ns dead time," *IEEE J. Sel. Topics Quantum Electron.*, vol. 28, no. 2, Mar./Apr. 2021, Art. no. 3800809.
- [9] C. Niclass and M. Soga, "A miniature actively recharged single-photon detector free of afterpulsing effects with 6Ns dead time in a 0.18 $\mu$ m CMOS technology," in *Proc. Int. Electron Devices Meeting*, 2010, pp. 14.3.1–14.3.4.
- [10] F. Severini et al., "SPAD pixel with Sub-NS dead-time for high-count rate applications," *IEEE J. Sel. Topics Quantum Electron.*, vol. 28, no. 2, Mar./Apr. 2022, Art. no. 3802808.
- [11] A. Giudici, G. Acconcia, I. Labanca, M. Ghioni, and I. Rech, "4 ns dead time with a fully integrated active quenching circuit driving a custom single photon avalanche diode," *Rev. Sci. Instrum.*, vol. 93, no. 4, Apr. 2022, Art. no. 043103.

- [12] W. Hwang, D. Kim, S. Moon, and D. Y. Kim, "Achieving a high photon rate in digital time-correlated single photon counting using a hybrid photodetector," *Opt. Exp.*, vol. 29, no. 7, pp. 9797–9804, Mar. 2021.
- [13] T. A. Abbas et al., "A CMOS SPAD sensor with a multi-event folded flash time-to-digital converter for ultra-fast optical transient capture," *IEEE Sensors J.*, vol. 18, no. 8, pp. 3163–3173, Apr. 2018.
- [14] A. C. Ulku, C. Bruschini, S. Weiss, X. Michalet, and E. Charbon, "A time-gated large-array SPAD camera for picosecond resolution real-time FLIM (Conference Presentation)," *Proc. SPIE*, vol. 10498, 2018, Art. no. 104980M.
- [15] M. Wahl et al., "Integrated multichannel photon timing instrument with very short dead time and high throughput," *Rev. Sci. Instrum.*, vol. 84, no. 4, Apr. 2013, Art. no. 043102.
- [16] A. Cominelli, G. Acconcia, P. Peronio, I. Rech, and M. Ghioni, "Readout architectures for high efficiency in time-correlated single photon counting experiments—Analysis and review," *IEEE Photon. J.*, vol. 9, no. 3, Jun. 2017, Art. no. 3900615.
- [17] A. Cominelli, G. Acconcia, P. Peronio, M. Ghioni, and I. Rech, "High-speed and low-distortion solution for time-correlated single photon counting measurements: A theoretical analysis," *Rev. Sci. Instrum.*, vol. 88, no. 12, Dec. 2017, Art. no. 123701.
- [18] S. Farina et al., "Above pile-up fluorescence microscopy with a 32Mc/s single-channel time-resolved SPAD system," *Opt. Lett.*, vol. 47, no. 1, pp. 82–85, Jan. 2022.
- [19] M. Patting et al., "Fluorescence decay data analysis correcting for detector pulse pile-up at very high count rates," *Proc. SPIE*, vol. 57, no. 3, Jan. 2018, Art. no. 031305.
- [20] S. Farina, G. Acconcia, I. Labanca, M. Ghioni, and I. Rech, "Toward ultra-fast time-correlated single-photon counting: A compact module to surpass the pile-up limit," *Rev. Sci. Instrum.*, vol. 92, no. 6, Jun. 2021, Art. no. 063702.
- [21] Y. Li et al., "Investigations on average fluorescence lifetimes for visualizing multi-exponential decays," *Front. Phys.*, vol. 8, Oct. 2020, Art. no. 576862.
- [22] T. Rebafka, F. Roueff, and A. Souloumiac, "Method for estimating parameters of the distribution of particle response times of a system, in particular applied to fluorescence measurements," French Patent Request 2010/089 363, Aug. 12, 2010.
- [23] A. Cominelli, "High-speed, low-distortion solutions for time-correlated single photon counting measurements," Ph.D. dissertation, Politecnico di Milano, Milan, Italy, Mar. 2019. [Online]. Available: <https://www.politesi.polimi.it/handle/10589/145767>
- [24] S. Cova, M. Ghioni, A. Lotito, I. Rech, and F. Zappa, "Evolution and prospects for single-photon avalanche diodes and quenching circuits," *J. Modern Opt.*, vol. 51, no. 9/10, pp. 1267–1288, Jul. 2004.
- [25] A. Gulinatti, I. Rech, M. Assanelli, M. Ghioni, and S. Cova, "A physically based model for evaluating the photon detection efficiency and the temporal response of SPAD detectors," *J. Modern Opt.*, vol. 58, no. 3/4, pp. 210–224, Feb. 2011.



**Ivan Rech** (Senior Member, IEEE) received the M.S. degree in electronic engineering and the Ph.D. degree (with Hons.) in information technology from the Politecnico di Milano, Milan, Italy, in 2000 and 2004, respectively. He is currently an Associate Professor with the Politecnico di Milano. He was involved in several interdisciplinary research projects on molecular biology, quantum cryptography, adaptive optics in astronomy, and developing dedicated instrumentation. His research interests include the development of single photon detectors and associated electronics

for biomedical, genetic, and diagnostic applications.



**Angela Bovolenta** (Graduate Student Member) received the B.S. degree in biomedical engineering and the M.S. degree (*cum laude*) in electronics engineering in 2019 and 2022, respectively, from the Politecnico di Milano, Milan, Italy, where she is currently working toward the Ph.D. degree in information technology, working on the design of new front-end circuits for Single-Photon Avalanche Diodes (SPADs), used in ultra-fast time-correlated single-photon counting (TCSPC) applications.



**Alessandro Cominelli** received the B.S. and M.S. degrees in electronics engineering from the Politecnico di Milano, Milan, Italy, in 2013 and 2015, respectively, and the Ph.D. degree in information technology from the Department of Electronics, Information and Bioengineering, Politecnico di Milano, in 2019, with the thesis "High-speed, low distortion solutions for Time-Correlated Single-Photon Counting (TCSPC) measurements. His main research interests include the design of high-performance integrated electronics for single-photon avalanche diodes (SPADs). He wrote several papers on this subject, including also theoretical analyses and improvement ideas for single-photon counting techniques, especially TCSPC.



**Giulia Acconcia** (Member, IEEE) received the B.S. degree in engineering of computing systems, the M.S. degree in electronics engineering, and the Ph.D. degree (with Hons.) in information technology from Politecnico di Milano, Milan, Italy, in 2011, 2013, and 2017, respectively. Since 2017, she has been with the Department of Electronics, Information and Bioengineering, Politecnico di Milano, where she is currently a Senior Researcher. She has coauthored more than 60 papers in international journals and conferences. Her research interests include the development of integrated electronics for high-performance counting and timing with Single Photon Avalanche Diodes (SPADs). Dr. Acconcia was the recipient of SPIE Rising Researcher in 2019 and Young Investigator Award in 2020.